Enhancements to the UK Photochemical Trajectory Model for Simulation of Secondary Inorganic Aerosol

Beddows, David; Hayman, Gary; Harrison, Roy

DOI:
10.1016/j.atmosenv.2012.04.020

Document Version
Early version, also known as pre-print

Citation for published version (Harvard):
Beddows, D, Hayman, G & Harrison, R 2012, 'Enhancements to the UK Photochemical Trajectory Model for Simulation of Secondary Inorganic Aerosol', *Atmospheric Environment*, vol. 57, pp. 278-288.
https://doi.org/10.1016/j.atmosenv.2012.04.020

ENHANCEMENTS TO THE UK PHOTOCHEMICAL TRAJECTORY MODEL FOR SIMULATION OF SECONDARY INORGANIC AEROSOL

DAVID C. S. BEDDOWS[1], GARRY HAYMAN[2] AND ROY M. HARRISON[1,1*] †

[1] National Centre for Atmospheric Science
School of Geography, Earth & Environmental Sciences
Division of Environmental Health & Risk Management
University of Birmingham, Edgbaston
Birmingham, B15 2TT, United Kingdom

[2] Centre for Ecology and Hydrology
Maclean Building, Benson Lane
Crowmarsh Gifford, Wallingford
Oxfordshire, OX10 8BB, United Kingdom

[*] To whom correspondence should be addressed (Tel: +44 121 414 3494; Fax: +44 121 414 3709; Email: r.m.harrison@bham.ac.uk)

[†]Also at: Department of Environmental Sciences / Center of Excellence in Environmental Studies, King Abdulaziz University, Jeddah, 21589, Saudi Arabia

Abstract

Particulate matter remains a challenging pollutant for air pollution control in the UK and across much of Europe. Particulate matter is a complex mixture of which secondary inorganic compounds (sulphates, nitrates) are a major component. This paper is concerned with taking a basic version of the UK Photochemical Trajectory Model and enhancing a number of features in the model in order to better represent boundary layer processes and to improve the description of secondary inorganic aerosol formation. The enhancements include an improved treatment of the boundary layer, deposition processes (both wet and dry), attenuation of photolysis rates by cloud cover, and inclusion of the aerosol thermodynamic model ISORROPIA II to account both for chemistry within the aerosol and between the particles and gas phase. Emissions inventories have been updated and are adjusted according to season, day of the week and hour of the day. Stack emissions from high level sources are now adjusted according to the height of the boundary layer and a scheme for generating marine aerosol has been included. The skill of the improved model has been evaluated through predictions of the concentrations of particulate chloride, nitrate and sulphate and the results show increased accuracy and lower mean bias. There is a much higher proportion of the values lying within a factor of 2 of the observed values compared to the basic model and Normalised Mean Bias has reduced by at least 89% for nitrate and sulphate. Similarly, the Index of Agreement between calculated and measured values has improved by ~10%. Considering the contribution of each enhancement to the improvement in the performance metrics, the most significant enhancement was the replacement of the parameterisation of the boundary layer height, relative humidity and temperature by HYSPLIT values calculated for each trajectory. The second most significant enhancement was the parameterisation of the photolysis rates by values calculated by an off line database accounting for the dependence of photolysis rates on zenith angle, cloud cover, land surface type and column ozone. The inclusion of initial conditions which were dependent on the starting point of the trajectory and the modulation of stack emissions made the most significant improvement to sulphate. Furthermore, in order to assess the model's response to abatement scenarios, 30% abatements of either NH_3, NO_x or SO_2 showed a reduction in the sum of chloride, nitrate and sulphate of between 3.1 % to 8.5 % (with a corresponding estimated reduction of 1.6 – 3.7% reduction in PM_{10}). The largest reduction in this contribution is due to the abatement of NO_x.

Keywords: Lagrangian model; sulphate; nitrate; chloride; Master Chemical Mechanism

Introduction

The United Kingdom, along with other European countries, is required to meet stringent air quality standards for PM_{10} and $PM_{2.5}$, as well as exposure reduction targets for $PM_{2.5}$ set by the European Union (EC, 2008). Abatement strategies to improve air quality with respect to particulate matter (PM) pollution have considerable economic cost. The Directive on "Ambient Air Quality and Cleaner Air for Europe" for example estimates the cost of the 'Maximum Technically Feasible Reduction' scenario, abating SO_2, NO_x, VOC, NH_3, and $PM_{2.5}$, to be € 39.7 billion per year in the year 2020. Additional measures may be needed as there has been little change in annual mean concentrations of PM_{10} since the year 2000 across considerable parts of Europe (Harrison et al., 2008, UN ECE report on PM, 2007: http://tarantula.nilu.no/projects/ccc/reports/cccr8-2007.pdf).

Airborne particulate matter, be it expressed as $PM_{2.5}$ or PM_{10} mass, is a complex mixture of chemical constituents. In the UK, the predominant individual constituents are sulphates, nitrates and organic matter. Campaign data was collected in the months of May and November of the years 2004 and 2005, in central Birmingham (Yin and Harrison, 2008), showing that sulphates and nitrates account on average for 34.5% of PM_{10} and 45.2% of $PM_{2.5}$ mass with the rest comprising of organics (PM_{10}; $PM_{2.5}$ = 23.7%; 26.1%), iron rich dust (PM_{10}; $PM_{2.5}$ = 13.4%; 5.9%), elemental carbon (PM_{10}; $PM_{2.5}$ = 8%; 11.2%), sodium chloride (PM_{10}; $PM_{2.5}$ = 9.3; 4%) and calcium salts (PM_{10};$PM_{2.5}$ = 7.4%; 2.5%). During episodes of elevated PM concentrations exceeding the daily European Limit Value of 50 μg m^{-3}, the contribution of sulphates and nitrates increased to 57.2% of PM_{10} and 68.5% of $PM_{2.5}$ (Yin and Harrison, 2008) and were associated with transport of secondary pollutants. Consequently, abatement of these components is potentially an attractive policy option focussing on their precursor gases emitted by traffic, industry and domestic sources (Erisman and Schaap, 2004, AQEG, 2005, Jones and Harrison, 2011).

Numerical models have an important part to play in predicting the impact of abatement strategies and a number of such models have been used to predict concentrations of particulate matter components within the European atmosphere. These include Eulerian models such as LOTOS-EUROS (Schaap et al., 2008), CHIMERE (Bessagnet et al., 2009), REM-CALGRID model (RCG) (Beekmann et al., 2007), and the Unified EMEP model (Simpson et al. 2011) to name but a few. The unified EMEP model has been used for policy development in Europe (Aas et al., 2007) to address regional scale impacts of NO_x and SO_2 emission reductions on PM mass concentrations (despite having uncertainties of about ± 40% for nitrate).

In the UK, the Photochemical Trajectory Model (PTM) has often been used to understand boundary-layer pollution. For example, Walker et al. (2009) and Baker (2010) simulated concentrations of ozone, and Derwent et al. (2009b) modelled concentrations of sulphate and nitrate. The PTM is a boundary-layer Lagrangian model whose main advantage over the Eulerian modelling approach is its ability to run highly comprehensive chemical schemes without simplifications and parameterisations that may compromise the performance of the chemical reaction scheme. The PTM is therefore suited to the examination of abatement policies aimed at targeting emissions of individual precursors (e.g. NH_3, NO_x, SO_2). A number of studies have modelled particulate matter in Europe. Most notably, the CityDelta project compared the ability of several models to predict the impact of emissions reductions upon concentrations in European cities (Cuvelier et al., 2007), specifically Berlin, Milan, Paris and Prague (Thunis et al., 2007). A subsequent study (Stern et al., 2008) examined the ability of five chemical transport models to reproduce PM_{10} episode conditions in central Europe. Model specific studies, such as those with CHIMERE, have sought to simulate particulate matter concentrations in specific parts of Europe, e.g. Portugal (Monteiro et al., 2007) and northern Italy (de Meij et al., 2009). Air quality models used for calculating aerosol species over the UK include the Community Multiscale Air Quality model (CMAQ), Chemel et al., 2010) and the Hull Acid Rain Model (HARM), (Metcalfe et al., 2005). CMAQ over-predicted O_3 and under-predicted aerosol species with the exception of sulphate (Chemel et al., 2010). The HARM and ELMO models (Whyatt et al., 2007) underestimated sulphate, nitrate and ammonium by a large margin, and chloride massively. In the work of Redington and Derwent (2002), the NAME model slightly under-predicted measured sulphate values although the annual average values of nitrate compared well.

We have previously used the UK Photochemical Trajectory Model (a version of the Derwent et al. (2009b) UK-PTM) to model concentrations of particulate sulphate and nitrate in southern England and Northern Ireland in 2002 (Abdalmogith et al., 2006). While our study was quite successful in modelling monthly mean concentrations and trends in both nitrate and sulphate, it performed poorly in modelling daily concentration data, especially during nitrate and sulphate episodes which were observed during easterly transport trajectory events that brought high levels of particulate matter from Europe. It was concluded that this was unlikely to be due to errors in the back trajectory alone and that inclusion of a more sophisticated treatment of emissions and meteorology would probably be required to address the issue adequately. It was also recognised that it would be advantageous to: (i) use more than one photochemical back trajectory calculation for

each daily measurement, (ii) update emissions inventories and injection parameters to account for daily and seasonal variation; (ii) add wet deposition processes; (iii) replace the dynamic approach which treated the chemistry of the NH_4NO_3 –HNO_3 –NH_3 system as a bimolecular gas phase reaction with a more sophisticated thermodynamic algorithm, ISORROPIA II and (iii) and replace the clear-sky photolysis rates with ones which accounted for cloud cover.

Numerous amendments have been applied to the original model to form an enhanced UK-PTM with a view to providing an improved model aimed at addressing policymaking decisions. In this paper, we assess the changes resulting from the enhancements by using observed gas- and aerosol-phase data collected at the Harwell observatory in Oxfordshire, UK in 2007.

TECHNICAL DESCRIPTION OF THE MODIFICATIONS TO THE UK-PTM

The UK-PTM is a boundary-layer trajectory model originally assembled to simulate photochemical ozone production and subsequently used to derive Photochemical Ozone Creation Potentials (POCPs) (Derwent et al., 1998, Derwent et al., 2005). The model was initially set up to represent an idealised summertime photochemical episode occurring over the UK and used linear air mass trajectories. More recent studies have used air mass back trajectories calculated from meteorological wind velocity vector fields and a parameterised boundary layer height (Abdalmogith et al., 2006; Derwent et al., 2009b; Walker et al., 2009 and Baker, 2010). The changes made by these authors have improved the PTM. Here, we have modified the PTM further to include a new treatment of aerosol processes and of emissions from tall stacks, the effect of cloud cover on photolysis values, wet deposition, and a revised treatment of the emissions, amongst others. A complete list of changes made to the emissions inventories, chemical mechanism and back trajectory calculation is presented in Table 1.

Initial Conditions

An implicit assumption made in the original model (Abdalmogith et al., 2006) was that all trajectories, if they were extrapolated far enough back in time, would start over the Atlantic. The initial conditions were fixed to one set of values derived from a remote marine location off the west coast of the Republic of Ireland. In practice, 3-5 day back trajectories with arrival points in the UK do not all start over the Atlantic but may start over continental Europe. Stohl (1998) recommends that these trajectories are not further lengthened in order to maintain a reasonable level of certainty of their position. The

amended model uses 5 starting regions, namely Western, Northern, Eastern, Southern and Central (Figure 1) to which initial concentrations of HCl, NO, NO_2, NO_3, HNO_3, SO_2, SO_4, CO, CO_2, CH_4, HCHO, O_3, NH_3, NH_4^+, NO_3^- and SO_4^{2-} were assigned (see Table S1 in Supplementary Information). These initial concentrations were derived from data measured at Birkenes, Braganca, Campisabolos, Glashaboy, Hohenpeissenberg, Ispra, Melpitz, Montelibretti, Norway Ocean Station, and S. Pietro Capofiume between 2000 and 2007. The initial concentrations were averaged over the measurements taken at a site which best represented the conditions within the initial zone, e.g. for the Western or Northern initial conditions, the most representative measurements are those collected at Birkenes with back-trajectories crossing only over the ocean or the polar ice cap. There is scope in the future to increase the number of starting zones and to make seasonal adjustments to these values or to use concentration fields provided from larger domain models.

Meteorology

The majority of studies use back trajectories with a timescale of 3-5 days. This is generally a compromise between having sufficient time to describe the long-range transport and the decreasing accuracy of individual back trajectories the further they are projected backward in time (Stohl, 1998). In this work, four-day back trajectories were calculated using the NOAA Hybrid Single Particle Lagrangian Integrated Trajectory (HYSPLIT-4) model (Draxler and Hess, 1998) and the archived NCEP/NCAR global data assimilation system data (GDAS). The original UK PTM was simply based on three day ECMWF back trajectories consisting of latitude/longitude values calculated online by BADC.

An improvement in accuracy can also be achieved by averaging over the values obtained from the output of more than one photochemical back trajectory for each daily PM measurement. Instead of using a single trajectory with a specific arrival time e.g. during the mid-afternoon at 15:00 h (as in the case of Baker (2010) who considered air parcel trajectories arriving in Birmingham, UK), our model was adapted to run photochemical calculations along trajectories for air masses arriving every hour of the day. This implied that for each daily PM_{10} filter measurement, an average calculated value was determined based on meteorological conditions which were liable to change significantly over the course of a day. Other multiple trajectory sampling schemes can potentially use trajectories arriving at different heights and/or at many nodes of a gridded zone placed symmetrically around the receptor site (private communication with R. Derwent, 2008).

In addition to latitude and longitude, other parameters are included in the back trajectory data, namely the boundary layer height, relative humidity and temperature. The HYSPLIT boundary layer heights give a more realistic description of the boundary-layer (BL) and replace the “clipped saw-tooth” function used in the earlier model of Abdalmogith et al. (2006) and shown in Figure S4 which is based on an idealised summertime episode. In particular, in HYSPLIT, the height of the mixing layer is taken as the height at which the potential temperature is at least two degrees greater than the minimum potential temperature. When plotted, the temporal boundary layer height profiles are no longer angular, they change more progressively and they are correctly synchronised to the rising and falling of the sun no matter at what latitude the air mass is located at. As the boundary layer expands, the constituents in the supra layer are mixed into the boundary layer and at dusk the supra layer concentrations are made equal to the boundary layer concentrations at dusk. However, as the boundary layer depth decreases, the constituents in the boundary layer are mixed back into the supra layer. There is no chemical evolution of the upper box.

Further auxiliary values in the back trajectory data included the 10 m wind velocity U_{10} and hourly rain rates f which were inputted into the parameterisation of sea salt flux and PM deposition respectively. Cloud cover and time/date data are also included so that the clear-sky assumption could be removed from the model and the emission flux corrections could be correctly synchronised to the hour of the day, day of the week and month of the year.

Chemistry

In order to include a more sophisticated treatment of aerosol properties (e.g. inclusion of ISORROPIA II) and to speed up the calculation, the Master Chemical Mechanism (MCM 3.1) was replaced with the Common Reactive Intermediate (CRI) mechanism (version CRI v02) developed by Jenkin et al. (2008). Jenkin et al. (2008) have shown that the CRI mechanism is virtually equivalent to the full MCM. This reduction in the number of species and reactions reduced the calculation time for one trajectory from one hour to approximately one minute. Watson et al. (2008) have made further reductions in the CRI mechanism by removing specific VOCs and reallocating the emissions to retained VOCs, but these reduced mechanisms were not included.

The VOC speciation used in this study is based on the speciated VOC emission inventory for 2000 compiled by Passant (2002) as part of the UK National Atmospheric Emission Inventory (NAEI) programme for the 2002 inventory year (the latest available at

the time of the original model development). This speciated emission inventory comprised 664 VOCs emitted from 249 source sectors with a total annual emission of 1543.7 ktonnes, including natural VOC emissions of 178 ktonnes per annum. The emissions from the 249 source sectors were aggregated to the relevant SNAP-1 sector. As many of the VOCs in the UK inventory were isomers or related to the model VOCs, the assignments were relatively straightforward.

In the original model, a clear sky scenario was always in place generally limiting the application of the model to summer conditions. The photolysis values J were parameterised to the solar zenith angle Z, using equation 1, where l, m, n, are constants available from the MCM website (http://mcm.leeds.ac.uk/MCM).

$$J = l(cosZ)^m \exp(-n \sec Z) \quad (1)$$

In the enhancement, the photodissociation rates were calculated off line using the PHOTOL code (Hough, 1988). This has been updated to account for changes to spectroscopic and photochemical parameters, most notably the quantum yield of ozone (Atkinson et al., 1997). The input database contains the dependence of photolysis rates for 21 species on zenith angle, cloud cover, land surface type and column ozone. The local photolysis rates were derived during the model run by identifying the nearest element in the database. The aerosol and ozone columns were initially fixed, the latter at ~300 DU, but could be varied subsequently. The tabular values not only accounted for the solar zenith angle at a given time of the day, latitude and longitude, but also account for the surface over which the air mass travels (surface albedo of land, sea or ice) and the fractional cloud cover which was included as a field within the back trajectory data. Fractional cloud cover values were extracted, for each step of the trajectory, from Global Data Assimilation System (GDAS) forecast data generated by the National Weather Service's National Centers for Environmental Prediction (NCEP) (http://ready.arl.noaa.gov/gdas1.php). Using this system, values of photosynthetically active radiation (PAR) are also derived for the calculation of an environmental correction factor for monoterpenes and isoprenes calculated in the biogenic emission inventories (Figure S5).

Aerosol Processes

In the original UK-PTM, the aerosol chemistry was accounted for by a very simple process to represent the establishment of thermodynamic equilibrium in the NH_4NO_3 – HNO_3 – NH_3 system. Ammonia was rapidly combined with available aerosol sulphate to

form ammonium sulphate and any ammonia that remained was assumed to form a thermodynamic equilibrium with nitric acid and ammonium nitrate. No account was taken of hygroscopic water uptake which substantially affects the equilibrium. Furthermore, the formation of coarse mode aerosol nitrate was parameterised by the reaction of N_2O_5 and nitric acid with natural dusts and sea salt. Abdalmogith et al. (2006) and Derwent et al. (2009b) provide more details. The parameterisations based on the concentrations of the trace gases NH_3, N_2O_5, HNO_3, and SO_3 have been replaced in the enhanced model by the aerosol thermodynamic equilibrium model for K^+, Ca^{2+}, Mg^{2+}, NH_4^+, Na^+, SO_4^{2-}, NO_3^-, Cl^-, H_2O aerosols and associated gases, called ISORROPIA II (Fountoukis et al., 2009). In this work, it was compiled from FORTRAN code into a dynamic link library accessible by the FACSIMILE model. The complete theory of ISORROPIA II, together with a detailed description of the equations solved, the activity coefficient calculation methods and the computational algorithms used can be found in Nenes et al. (1998a,b) and Fountoukis and Nenes (2007).

Aqueous Phase Processes

The aqueous phase oxidation of SO_2 to H_2SO_4 in clouds is treated using a pseudo first-order process with a reaction constant R_k. The original value for R_k based on an assumed conversion of 1-2% / hour was replaced by a parameterisation based on relative humidity and cloud cover ε, (see equation 2 and Schaap et al. (2004)).

$$R_k = \begin{cases} 5.8 \times 10^{-5}(1+2\varepsilon), & RH < 90\,\% \\ 5.8 \times 10^{-5}(1+2\varepsilon)[1.0 + 0.1 * (RH - 90.0)], & RH \geq 90\,\% \end{cases} \quad (2)$$

Deposition Values

The conventional resistance approach - reviewed by Wesely and Hicks (2000) - of representing dry deposition processes was used in the model. The rate of dry deposition of the chemical species *i*, of concentration *Ci*, was given by,

$$\frac{\mathrm{d}}{\mathrm{dt}}[C_i] = -\frac{v_g}{H}[C_i] \quad (3)$$

where the boundary layer height and deposition velocity are represented by H and v_g respectively. For gases, tabulated dry deposition values were subdivided in the model to account for whether the air mass was over land or sea (see Table S2). For ozone, a more developed representation was used which accounted for the diurnal and seasonal variation induced by stomatal opening and closing. In the model, the approximation of the half sinusoidal function described by Hayman et al. (2010) was used. Further

improvements could be made by accounting for the opening and closing of stomata in response to the availability of moisture and the meteorological conditions. This adjusts the deposition value of ozone between a night time and winter constant value of 2 mm s^{-1} and a seasonal maximum ranging from 4 to 7 mm s^{-1} (Hayman, 2010).

For particulate matter (in this case for chloride, nitrate and sulphate particles) dry-deposition was accounted for by an expression developed by Smith et al. (1993) primarily for air masses as they move over the sea (equation 4),

$$V_d = \frac{Vt}{1-\exp\{-\left(\frac{V_t}{CD \cdot U_{10}}\right)\}} \quad (4)$$

This is a function of the 10 m wind speed U_{10}, the gravitational sedimentation velocity V_t and the Drag Coefficient *CD,* between the atmosphere and ocean (equation 5).

$$CD(U_{10}) = \begin{cases} 1.14 \times 10^{-3}, & U_{10} \leq 10\, ms^{-1} \\ (0.49 + 0.065U_{10}) \times 10^{-3}, & U_{10} > 10\, ms^{-1} \end{cases} \quad (5)$$

This expression (eq. 4) was used for land multiplied by a ratio of typical fixed land/sea values for 1μm particles.

An additional loss term Λ_g, was added to represent removal by wet deposition using the parameterisation given by McMahon et al. (1979). This is a function of hourly rainfall f which was taken from the HYSPLIT back trajectory data (equation 6). The expression for SO_2 appears in equation 6, where *f* is the rainfall rate (mm h^{-1})

$$\Lambda_g = 17 \times 10^{-5} f^{0.6} \quad (6)$$

Emission Inventories

Emission fluxes were calculated using one of two sets of SO_2, NO_x, NMVOC, CO and NH_3 emission inventories. For the UK land mass, NAEI emission data were used (http://naei.defra.gov.uk/). The NAEI inventory programme produces annual emission maps at 1 km x 1 km spatial resolution for the major emission source sectors. These were aggregated to 10 km x 10 km for each pollutant and major source sector. Emission data were taken from EMEP (http://www.emep.int/) for the remaining model domain. These were available on a 50 km x 50 km grid for the same pollutants and major emission source sectors. The base year for the emissions was 2005 (the latest available at the time of the work), which were scaled to 2007 using the ratio of the national sector emission totals for 2005 and 2007 for each country. In a similar manner to that adopted by Hayman et al. (2010), a separate term was added to represent the emissions of VOCs from natural sources (taken to be trees), This is described further below.

Emission fluxes

Instantaneous emission fluxes were derived from the annual average emission inventories for SO_2, NO_x, CO, NH_3, VOCs and NMVOCs and updated every 30 minute trajectory step within the calculation as the air mass moved across the model domain. The emissions were calculated from the annual emissions of NH_3, NO_x, VOCs, biogenic VOCs, EC, and OC, scaled by factors describing diurnal, day-of-week, and monthly variations which were published as part of the City-Delta European Modelling Exercise (http://aqm.jrc.ec.europa.eu/citydelta/temp_factors_gh.txt)

Biogenic emission fluxes

Additional emission terms are added to the emission rate of isoprene and terpenes to represent the natural biogenic emissions from European forests and agricultural crops. The emission inventory used was that derived in the PELCOM project (PELCOM, 2000). The inventory was aggregated to the EMEP 50 km x 50 km grid and gives emission potentials for isoprene (from deciduous and evergreen trees: temperature and light-sensitive), monoterpenes (from deciduous and evergreen trees: temperature or temperature and light-sensitive) and other VOCs (OVOCs, from deciduous and evergreen trees: temperature sensitive). The emission potentials were converted to local emission rates using environmental correction factors (Guenther, 1997), derived from the meteorological datasets. Hayman et al. (2010) compared the PELCOM emission inventory with other estimates and discussed the implications of using this inventory.

Sea salt emission flux

In order to use ISORROPIA II, a sodium and chloride concentration were required and this was derived from a sea-salt parameterisation developed by Gong (2003). Figure S1 shows the flux distribution (equation 7) used to derive an injection term in the model which was dependent on the wind speed at 10 m (U_{10}). This term was integrated into a mass flux (using particle density to mass density relationship, $\frac{dm}{dr} = m_p \frac{dF}{dr}$) for all particle radii r, reducing the parameterisation to a term involving just U_{10},

$$\frac{dF}{dr} = 1.373 u_{10} r^{-A} (1 + 0.057 r^{3.45}) \times 10^{1.607 e^{-B^2}} \quad (7)$$

For values of particle radius r and an adjustable parameter $\Theta = 30$, which controls the shape of the sub-micron size distributions, the constants A and B are given by equations 8 and 9.

$$A = 4.7(1 + \Theta r)^{-0.017 r^{-1.44}} \quad (8)$$

$$B = (0.433 - log\, r)/0.43 \quad (9)$$

Treatment of emissions from large stacks

As the modelled air mass tracks along a trajectory, the emissions are entered independently of any height constraint into the boundary layer, suggesting a possible reason for the initially high SO_2 values (c.a. 2.5 times the expected value). Redington and Derwent (2002) also reported a similar problem with SO_2 concentrations calculated by their NAME model. The highest emissions of SO_2 on the emission maps were attributable to coal- and oil-fired power stations, together with other heavy industries (illustrated for the UK in Figure S3). Given that major industrial emissions are made via tall chimney stacks (100-300 m), there will be times of the day when the emissions are not made into the boundary layer but above it. Compared to state-of-the art 3-D models, where the emissions can be injected into the relevant model layer, this is a limitation of the boundary-layer model.

Bieser et al. (2011) calculated the vertical emission profiles of point-source emissions over Europe, evaluating an average effective emission height from plume rise calculations applied to various meteorological fields, seasons, times of the day and emission stack characteristics. In this work, an empirical equation (10) - approximating the findings of Bieser et al. (2011) - was derived by re-aggregating the calculated fractional values for the binned emission heights.

$$AFV(h) = \begin{cases} 0, & h < 144\,m \\ 0.45 + \tan^{-1}(1.02 * h - 310.6)/2.49, & 144\,m < h < 724\,m \\ 1, & h \geq 724\,m \end{cases} \quad (10)$$

where AFV(h) represents the mixing height (h)-dependent average fractional value of the emissions.

Using equation 10, the chimney code cuts the SNAP 1 NO_x and SO_2 emission fluxes by the fractional value AFV(h), if (i) the air mass passes over an emission square containing a major point source and (ii) the boundary layer height is less than 724 m, when it starts to slice the average emission plume.

The locations of emitting stacks were identified in the model using positional data published by the European Environment Agency's European Pollutant Release and Transfer Register (E-PRTR). (http://prtr.ec.europa.eu/) In total, 417 UK and 5171 European NO_x and SO_2 emitters are accounted for in this way within the model. The inclusion of a "chimney code" attempts to overcome the limitation of a single box to

describe the boundary layer. As a result, the relatively high NO_x and SO_2 concentrations are reduced by 69% and 91% on average respectively relative to the base case of 11.18 ppb and 2.43 ppb without the "chimney code". Future model enhancements may well seek to account for the seasonal and daily activity of the power stations according to expected output.

The main local source of SO_2 and NO_x within the vicinity of the Harwell site is Didcot power station which is an 1.9 GW coal fired station used to meet peak demand. This is located 7 km downwind of Harwell for the prevailing south-westerly air masses, and it has been shown in a past study (Jones and Harrison, 2011) that Didcot power station has virtually no influence on the measurements at Harwell, and thus the SO_2 and NO_X emissions are reduced to zero for Didcot Power station in the model. This conclusion was drawn from data collected at Harwell from 2001 to 2008 and is thought to be due primarily to the lofting of the chimney emissions above the air sampled at Harwell.

Computation

The model was coded using the FACSIMILE numerical integration package (Curtis and Sweetenham, 1988). For each species *i* within the air parcel, its concentration within the boundary-layer C_i is governed by the differential equation (11)

$$\frac{\mathrm{d}}{\mathrm{dt}}[C_i] = P_i + \frac{E_i}{H} - L_i[C_i] - \frac{v_g}{H}[C_i] - ([C_i] - [B_i])\frac{1}{H}\frac{\mathrm{dH}}{\mathrm{dt}} \quad (11)$$

The source terms include the local emission rate from pollution sources E_i and the production rate of the species from photochemistry P_i. Similarly, the loss terms include the loss rate by photochemistry L_iC_i and dry deposition rate $\frac{\mathrm{v_g}}{\mathrm{H}}[\mathrm{C_i}]$. The effect of boundary layer height changes is represented by the time-dependent variable *H*. B_i is the concentration of the species in the supra boundary layer. The differential equations were solved using the variable order GEAR solver in the FACSIMILE software package.

Model Validation

The model was used to simulate a wide range of PM concentrations measured at the Harwell site in southern England (latitude = 51.571ºN and longitude = 1.325ºW). The primary test of the model was against daily concentrations of chloride, nitrate and sulphate collected at the Harwell site as part of the Airborne Particle Concentrations and Numbers Network (Hayman, 2008). The daily samples were collected using a Partisol 2025 sampler fitted with a PM_{10} inlet. In addition hourly concentrations of NO, NO_x, CO and O_3 data were measured using chemiluminescence, IR Absorption and UV absorption respectively. The

data are verified and ratified every quarter using the results from independent QA/QC site audits (see link for more details http://www.airquality.co.uk/verification_and_ratification.php).

Other analytes were taken from other networks offering either a monthly or an hourly resolution. Monthly measured data was taken from the Acid Gas and Aerosol Network (AGANET) and the National Ammonia Monitoring Network (NAMN). These are two of the four components of the UK Eutrophying and Acidifying Atmospheric Pollutants (UKEAP) network (http://pollutantdeposition.defra.gov.uk/aganet). The UKEAP measurements were carried out using the CEH DELTA (DEnuder for Long-Term Atmospheric sampling) system which is a low-cost diffusion denuder system that was originally developed for long-term sampling of ammonia and ammonium (Sutton et al., 2001), and which has also been tested for long-term sampling of acid gases (HNO_3, HONO, HCl, SO_2) and aerosols (NO_3^- NO_2^-, Cl^-, SO_4^{2-}) (Tang et al., 2008). Quality Assurance is maintained through the implementation of established sampling protocols, and monitoring of laboratory performance through participation in the EMEP and WMO-GAW inter-comparison schemes for analytical laboratories. The data quality is assessed using set Quality Control criteria: a) based on the capture efficiency using two denuders in the DELTA systems and b) involving the coefficient of variation for ammonia concentrations with the triplicate ALPHA samplers. Further details of the measurements and verification/ratification procedures are given in the annual reports to DEFRA (see link http://www.uk-pollutantdeposition.ceh.ac.uk/reports).

RESULTS

Generalisation of the Patterns Observed in the Daily Back Trajectories

Data from the period 19 March 2007 to 18 May 2007 were used for the validation capturing a large range of PM_{10} values to model. The patterns observed in the measured daily PM values can be accounted for by how the 24 hourly back trajectories (for the measurement day) spread across the emission map (see Figure S6). At the start of the sampling period (19th March) an increase – from relatively small concentrations - in the nitrate and sulphate values - was observed after the third day (Figure 2). This is accounted for by the air mass trajectories switching their origins from over the North Pole (passing directly down through Scotland and Northern England to the receptor site on 20/03/2007) to an origin in Eastern Europe on 25th March (25/03/2007 in Figure S6). The air masses continued to originate from eastern Europe up until 2nd April (03/04/2007) after which the starting points of the trajectories move towards the North Sea and then towards

458 the Atlantic off the coast of Republic of Ireland and France between 3rd and 14th April
459 (09/04/2007). From 15th April to 5th May the trajectories start at locations close to the west
460 and east coast of the UK, crossing over France, Germany and Denmark periodically
461 (15/04/2007). Then in the final phase of the sampling period 6-19th May, the air masses
462 have their origin firmly in the middle of the Atlantic Ocean (18/05/2007). In general, when
463 the air mass spends most of its time over the sea, the chloride measurements are high
464 and the nitrate and sulphate are low (see Figure 2). Conversely, when the air mass
465 originates over land and passes mainly over land, then the chloride measurements are low
466 and the nitrate and sulphate measurements are high, consistent with the clustered back
467 trajectory measurements of Abdalmogith and Harrison (2005). When considering the time
468 series of predicted and modelled chloride, nitrate and sulphate, the model output
469 impressively tracks the measured nitrate values. Similarly, the modelled sulphate values
470 satisfactorily track the measured values but with a high degree of scatter shown by the
471 plotted hinges. The performance of chloride is not as impressive but is acceptable when
472 considered in the context of the range of modelled values with nitrate and sulphate.
473

474 **Model Verification and Validation**

475 Table 2 compares the simple statistical values calculated for the gases $NH_{3(g)}$, HNO_3,
476 SO_2, HCl, CO, NO, NO_2 and O_3 and the aerosol components NH_4^+, Cl^-, NO_3^-, SO_4^{2-}, for the
477 period 02/04/2007 to 30/04/2007, across which the average temperature and relative
478 humidity were 11^oC and 72 % respectively. This period corresponds to the monthly
479 denuder and aerosol filter measurement for April made on the Acid, Gases and Aerosol
480 Network (AGANET). Considering the core functionality of the enhanced-PTM in
481 predicting ozone, the model under-predicts O_3, NO and NO_2 by 20%, 64% and 46%
482 although the ratio of NO_2 to NO is similar for both modelled and measured values.

483 The enhanced model under-predicts mean values of ammonia gas, ammonium, nitric
484 acid and hydrochloric acid by 12 %, 0 %, 88 % and 96 % respectively. In the original
485 model, there was an overestimation of sulphur dioxide as also reported by Redington and
486 Derwent (2002). By using the height dependent emission of SO_2, prescribed in the
487 chimney code, we have brought this prediction down from a mean value of 2.43 ppb to a
488 mean value of 0.27 ppb. With regards to the particulate matter concentrations, the model
489 over-predicts the measured value of chloride, nitrate and sulphate by 20 %, 8.1 % and
490 18% respectively. Although these discrepancies appear large, the model results appear
491 more reasonable when comparing with the full time series (Figure 2 & 3).

The improvement in the capability of the enhanced PTM to model nitrate and sulphate can be judged from Figure 2 where a comparison with the original model output is presented. Both original and enhanced modelled values of nitrate and sulphate do indeed span the range of measured values for the sampling period considered but the original model fails to account for specific scenarios thus leading to a short-fall in the calculated nitrate and sulphate values. The original model did not calculated chloride but the comparison shows that the enhancements made to the model address the general under prediction of nitrate and sulphate. The original PTM was capable of modelling the more significant nitrate and sulphate episodes associated with easterly back trajectories but failed to account for the smaller episodes resulting from westerly trajectories. This led to sharp increases in nitrate and sulphate when the air masses switched from westerly to easterly (14/04/2007-15/04/2007). The enhanced model accounts better for the high values observed during the nitrate episodes, especially the episode between 25th and 27th March where the nitrate value reached 36 μg m^{-3}. This episode was initially thought to be due to the presence of fog, although the meteorology measured at the nearby met-station of Benson did not indicate this to be the case. However, weather diaries for these three days record the UK weather as being generally dry by day due to an anticyclonic ridge, which can be associated with overnight fog. (see link: http://www.met.rdg.ac.uk/~brugge/diary2007.html). The trajectories for this period originated over central and eastern Europe thus leading to the observed sulphate episode. The enhanced model also reflected, but over-predicted, later sulphate episodes (12/04/2007-18/04/2007 and (20/04/2007-24/04/2007). Whereas the original model represented this episode by a brief spike in the sulphate values, the new model, which is able to model episodes due to westerly air masses, shows a longer episode better matching the measured data.

A direct comparison of the calculated and measured data is shown in Figure 3 where the time-series data has been replotted. The poor performance of the model to account for chloride can be immediately seen by the large fraction of points which are respectively either above or below the marked 2:1 or 1:2 boundary. Although the general trend is correct, there is a significant amount of scatter about the fitted and 1:1 line showing that there is a weakness in the modelling of chloride to be accounted for. The plots for nitrate and sulphate are much better with the majority of points within the 2:1 and 1:2 boundary. The over-prediction of sulphate results in a larger than unity gradient for sulphate, and the less than unity gradient of nitrate suggest the model is still slightly under-estimating the

higher values seen during the episodes.

Even though some of the higher measured chloride values are under-predicted, the temporal trends predicted by the model reflect the measured values fairly well as seen in Figure 2. This gives confidence in the ability of the Gong parameterisation and ISORROPIA II parameterisation to model the correct magnitude of sea salt, although the measured value was in general within or just outside of the max/min modelled values. This large discrepancy may be accounted for by uncertainties in the trajectory values of 10 m wind speed. Good results are obtained for nitrate for which the median daily value was much closer to the PM value. With regards to sulphate, the PTM was able to model correctly both high and low sulphate episodes although with a very high scatter of values as depicted by the max/min point of the plotted hinges. Also, there were periods where sulphate was significantly over-predicted.

Table 3 considers the effect of the model enhancements - measured against the daily observed PM measured values - using performance metrics calculated separately for the original and enhanced UK-PTM. The complete 61 day measurement period was considered for this comparison and the enhanced model improves considerably the average calculated values for the period. Both nitrate and sulphate were under-predicted relative to the observed values by 56% using the original model. The enhancements reduced this discrepancy for nitrate and sulphate to within 1.5% and 3.3% of the measured mean values and the calculated chloride value was within 13% of the measured value. Furthermore, improvements in how well the calculated values track with the measured values are reflected in the values of Spearman's correlation coefficient r which increase from approximately 0.5 to 0.83 and 0.65 for nitrate and sulphate respectively. As Figure 3 also indicates, the correlation coefficient of 0.5 for the chloride values shows that the model does not estimate chloride as well as it calculates nitrate and sulphate.

The Root Mean Square Error, RMSE provides information on the short term performance and has a possible range from 0 to $+\infty$ (Derwent 2009a). Again, the closer this value is to zero the better is the short term performance and although fractional values are not achieved using the enhanced model and we do not better the values of Derwent et al. (2009b) modelling longer time series measurements at Harwell with a UK-PTM, a considerable improvement in the short term performance of the PTM can be seen in our enhanced model. The Index of Agreement, IA, reflects the improvement in performance. IA is a statistical measure of the correlation of the predicted and measured concentration; the closer this is to 1 the better the correlation. For nitrate and sulphate an increase in the

560 value of IA is observed from 0.88 and 0.86 to 0.96 and 0.95 respectively. The value of IA
561 for chloride is also unexpectedly high considering the values of Spearman correlation
562 coefficient (r). As argued by Nath and Patil (2006) the value of r is often misleading as it
563 may be unrelated to the size of difference between observed and predicted values, and
564 that IA is better measure of how two values track each other over a period of time.
565 The improvement in the calculation of nitrate and sulphate is reflected also in the
566 improved value of the mean bias error MB. The Mean Bias, MB provides information on
567 the long term performance and has a range between the negative of the mean observed
568 value to $+\infty$. The closer this value is towards zero the better the long term performance.
569 For both nitrate and sulphate the MB value is reduced to fractional values implying that the
570 model's long term performance is improved. The fractional MB value for chloride also
571 indicates that the model's long term performance in calculating chloride is comparable to
572 that of nitrate and sulphate. Considering the Normalised Mean Bias (NMB) values, if these
573 lie between -0.2 and 0.2 then the model is acceptable according to the recommendation of
574 Derwent et al. (2009a). For the case of the nitrate and sulphate values respectively, the
575 values decrease in magnitude from -0.59 and -0.58 respectively using the original model to
576 0.05 and -0.07 for the enhanced model (cf the average values of Derwent et al. (2009a) of
577 0.05 and 0.14 for the whole year). The NMB value of -0.1 for chloride indicates that the
578 model's performance is acceptable but far from ideal. This is also reflected by the fraction
579 of the calculated chloride concentrations FAC2, within a factor of two of the observed
580 values, being just less than 50 %. For nitrate and sulphate this FAC2 value is 77 % and 81
581 % respectively. Using the original model the fraction of calculated nitrate and sulphate
582 values within a factor of 2 of the observed values was 18% and 11% respectively.
583 The contribution of each enhancement can be judged in Table 4. In this, the results
584 from the enhanced model are compared with the chloride, nitrate and sulphate values
585 when each enhancement is restored to its original setting. For each case, the decrease in
586 performance is represented by each percentage. Considering the percentage change in
587 the arithmetic means, the significance of the enhancements has been ranked from top to
588 bottom in the table. The most significant enhancement for chloride, nitrate and sulphate is
589 observed when the replacement of parameterisation of temperature, relative humidity and
590 the boundary layer height by values modelled by HYSPLIT. This is closely followed by the
591 enhanced photolysis values for just chloride and nitrate and then by the inclusion of
592 ISORROPIA II and cloud cover in the model for nitrate. The enhancement of the liquid
593 phase oxidation of SO_2 to H_2SO_4 in clouds by equation 2, inclusion of stack height
594 dependent emissions and the improvement in the initial conditions contribute most to the

595 sulphate enhancement. These trends are also observed with the percentage change of
596 the NMB values and in the context of a limit of acceptability of ±0.2, the largest changes
597 were seen for sulphate. Similar comparisons were made for FAC2 and r^2 and although the
598 changes were not as significant, again, the maximum changes were observed for
599 sulphate.

600 For policymaking decisions, Derwent et al. (2009b) showed that a 30% abatement of
601 either NH_3, NO_x or SO_2 led to at least 3,5% reduction of either nitrate or sulphate.
602 Reducing NH_3 by 30% reduced nitrate and sulphate by 12.2% and 0% respectively
603 compared to a 14.8% and 2.3% reduction when abating NO_2 (Derwent et al., 2009b). The
604 abatement of SO_2 yielded the highest reduction (of 14.8%) of the contribution of sulphate
605 to the PM value. The abatement of CO had no effect on the PM contribution from
606 ammonium, nitrate or sulphate. Likewise, the abatement of VOCs reduced the
607 contribution to PM from ammonium, nitrate and sulphate by 0 %, 2.1 % and 0.6 %
608 respectively. Referring to Table 5, our model shows comparable findings. Abating NH_3 by
609 30 % reduced nitrate and sulphate by 5.1 % and 0.1 % respectively. Similarly, lowering
610 NO_X by 30 % reduced nitrate and sulphate by 17.7 % and 1.9 % respectively. The 30 %
611 abatement of SO_2 yielded the highest reduction (by 20.8 %) of the contribution to the PM
612 value via sulphate and 2.5% of nitrate. For NO_X and SO_2, our enhanced model predicts a
613 larger reduction of nitrate and sulphate respectively, compared to Derwent et al. (2009b)
614 suggesting that our enhancements are potentially accounting for additional sensitivity to
615 the abatement of these precursors. The model suggests that the abatement of any of NH_3,
616 NO_x, or SO_2 by 30% will lead to a reduction in the sum of SO_4^{2-}, NO_3^- and Cl^- of between
617 3.1 % to 8.5 %, with the largest reduction due to NO_x abatement.

618

619 **SUMMARY**

620 Modifications to the UK Photochemical Trajectory model have been made in order to
621 make the chemical and meteorological processes more representative of the actual
622 conditions leading to the composition of the air masses sampled. The principal aim of this
623 work has been to model values of chloride, nitrate and sulphate over a fixed period of time
624 where a varied range of hourly nitrate values have been encountered resulting from air
625 mass trajectories with origins both over sea and continental Europe. Although the full
626 episodic trends of nitrate have not been totally accounted for by the enhancement, the
627 nitrate, sulphate and chloride have been modelled far more satisfactorily in comparison to
628 the original model.

When the original and enhanced UK-PTM are evaluated against the criteria established by Derwent et al. (2009a) for deciding the adequacy of models for policy relevant queries, we observe a general improvement in the performance metrics. The largest improvement is seen for the nitrate concentration with the mean bias falling to well below 0.05 with 77 % of the values lying within a factor of two of the observed values. The calculations of sulphate had a mean bias of 0.07, and 88 % of the values lay within a factor of two of the observed values. The calculation of chloride however needs improvement having a normalised mean bias of -0.1 with 42 % of the calculated values lying within a factor of two of the observed values. In general, the original model under predicted the average observed values by 55% and using the enhancements the model calculates nitrate and sulphate to within 1.5% and 3.3% of the mean measured values. Furthermore, the enhancements have improved the correlation between the calculated and measured values reflected by the increase in the Index of Agreement from 0.88 and 0.86 to 0.96 and 0.95 for nitrate and sulphate respectively. Similarly, improvements in the model's ability to represent the long and short term trends in both nitrate and sulphate have been demonstrated by the lowering of the values of the normalised mean bias and root mean square error towards the preferred values of zero. Our model indicates that a 30% abatement of either NH_3, NO_x or SO_2, will lead to a reduction in the sum of chloride, nitrate and sulphate of between 3.1 % to 8.5 % (with a corresponding estimated reduction of 1.6 – 3.7% reduction in PM_{10}). The largest reduction in this contribution is due to the abatement of NO_x.

ACKNOWLEDGEMENT

The National Centre for Atmospheric Science is funded by the U.K. Natural Environment Research Council. This work was also supported by the European Union EUCAARI (Contract Ref. 036833) and EUSAAR (Contract Ref. 026140) research projects, and by the U.K. Department of Environment, Food and Rural Affairs (Contract Ref. CPEA28).

REFERENCES

Aas, W., Bruckmann, P., Derwent, R., Poisson, N., Putaud, J.-P., Rouil, L., Vidic, S. and Karl-Espen Yttri, K.-E., 2007. EMEP Particulate Matter Assessment Report, EMEP/CCC-Report 8/2007, REF O-7726.

Abdalmogith, S.S. and Harrison, R.M.,2005. The use of trajectory cluster analysis to examine the long-range transport of secondary inorganic aerosol in the UK., Atmospheric Environment, 39, 6686-6695.

Abdalmogith, S.S., Harrison., R.M. and Derwent, R.G., 2006. Particulate sulphate and nitrate in Southern England and Northern Ireland during 2002/3 and its formation in a photochemical trajectory model, Science Total Environment, 368, 769-780.

AQEG,2005. Particulate Matter in the UK: Summary, Air Quality Expert Group, Defra, London.

Atkinson, R., 1997. Gas phase tropospheric chemistry of volatile organic compounds: 1. Alkanes and alkenes. Journal of Physical and Chemical Reference Data, 26, 215-290.

Ayers, G.P., 2001. Technical Note: Comment on Regression Analysis of Air Quality Data, Atmospheric Environment, 35, 2423-2425.

Baker, J., 2010. A cluster analysis of long range air transport pathways and associated pollutant concentrations with the UK, Atmospheric Environment, 44, 563-571.

Beekmann, M., Kerschbaumer, A., Reimer, E., Stern, R. and Moller, D., 2007. PM measurement campaign HOVERT in the Greater Berlin area: model evaluation with chemically specified observations for a one year period, Atmospheric Chemistry & Physics, 7, 55–68.

Bessagnet, B., Menut, L., Curci, G., Hodzic, B., Guillaume, A., Liousse, C., Moukhtar, S., Pun, B., Seigneur, C. and Schulz, M., 2009. Regional modeling of carbonaceous aerosols over Europe - Focus on Secondary Organic Aerosols. Journal of Atmospheric Chemistry, 61, 175–202.

Bieser, J., Aulinger, A., Matthias, V., Quante, M. and Denier van der Gon, H.A.C., 2011. Vertical emission profiles for Europe based on plume rise calculations. Environmental Pollution, 159, 2935-2946.

Chemel, C., Sokhi, R.S., Yu, Y., Hayman, G.D., Vincent,K.J., Dore, A.J., Tang,Y.S., Prain, H.D. and Fisher, B.E.A., 2010. Evaluation of a CMAQ simulation at high resolution over the UK for the calendar year 2003, Atmospheric Environment , 44, 2927-2939.

Cuvelier, C., Thunis, P., Vautard, R., Amann, M., Bessagnet, B., Bedogni, M., Berkowicz, R., Brant, J., Brocheton, F., Builtjes, P., Carnavale, C., Coppalle, A., Denby, B., Douros, J., Graf, A., Hellmuth, O., Hodzic, A., Honore, C., Jonson, J., Kerschbaumer, A., de Leeuw, F., Minguzzi, E., Moussiopoulos, N., Pertot, C., Peuch, V.H., Pirovano, G., Rouil, L., Sauter, F., Schaap, M., Stern, R., Tarrasonn, L., Bignati, E., Volta, M., White, L., Wind, P. and Zuber, A., 2007. CityDelta: A model intercomparsion study to explore the impact of emission reductions in European cities in 2010, Atmospheric Environment, 41, 189-207.

Curtis, A.R. and Sweetenham, W.P., 1988. FACSIMILE/CHEKMAT Users Manual. AERE Report R12805. Harwell Laboratory, Oxfordshire, UK.

Derwent, D., Fraser, A., Abbott, J., Jenkin, M., Willis, P. and Murrells T., 2009a. Evaluating the Performance of Air Quality Models, Report to the Department for Environment, Food and Rural Affairs, Welsh Assembly Government, the Scottish Executive and the Department of the Environment for Northern Ireland ED48749801 Issue 2.

Derwent, R., Witcham, C., Redington, A., Jenkin, M, Stedman, J., Yardley, R. and Hayman, G., 2009b. Particulate matter at a rural location in southern England during 2006: Model sensitivities to precursor emissions, Atmospheric Environment , 43, 689-696.

Derwent R.G., Jenkin M.E., Saunders S.M., Pilling M.J. and Passant N.R., 2005. Multi-day ozone formation of alkenes and carbonyls investigated with a Master Chemical Mechanism under European conditions., Atmospheric Environment , 39, 627-635.

Derwent, R.G., Jenkin, M.E., Saunders, S.M. and Pilling, M.J., 1998. Photochemical ozone creation potentials for organic compounds in North West Europe calculated with a Master Chemical Mechanism, Atmospheric Environment , 32, 2419-2441.

Draxler, R.R. and Hess, G.D., 1998. An overview of the HYSPLIT-4 modelling system for system for trajectories, dispersion and deposition, Australian Meteorological Magazine, 47, 295 -308.

EC, 2008. Directive 2008/50/EC of the European Parliament and of the Council of 21 May 2008 on Ambient air quality and cleaner air for Europe. Official Journal of the European Union, 11.6.2008, L 152/1.

Erisman, J.W. and Schaap M., 2004. The need for ammonia abatement with respect to secondary PM reductions in Europe, Environmental Pollutution, 129, 159–163.

Fountoukis, C. and Nenes, A., 2007. ISORROPIA II: A Computationally Efficient Aerosol Thermodynamic Equilibrium Model for K^+, Ca^{2+}, Mg^{2+}, NH^{4+}, Na^+, SO_4^{2-}, NO_3^-, Cl^-, H_2O Aerosols., Atmospheric Chemistry & Physics, 7, 4639–4659.

Fountoukis, C., Nenes, A., Sullivan, A., Weber, R., VanReken, T., Fischer, M., Matias, E., Moya, M. Farmer, D., and Cohen, R., 2009. Thermodynamic characterization of Mexico City Aerosol during MILAGRO 2006, Atmospheric Chemistry & Physics, 9, 2141-2156.

Gong, S.L., 2003. A parameterisation of sea-salt aerosol source function for sub- and super-micron particles, Global Biogeochemical Cycles, 17, 1097.

Guenther, A., 1997. Seasonal and spatial variations in natural volatile organic compound emissions. Applied Ecology 7, 34-45.

Harrison, R.M., Stedman, J. and Derwent, D., 2008. Why are PM_{10} concentrations in Europe not falling?, Atmospheric Environment, 42, 603-606.

Hayman, G., Yardley R., Quincey, P., Butterfield, D., Green, D., Alexander J., Johnson, P., Tremper A, (2008) NPL REPORT AS 25, CPEA 28: Airborne Particulate Concentrations and Numbers in the United Kingdom (phase 2) Annual Report - 2007 ISSN 1754-2928.

763 Hayman G.D., Abbott J., Davies, T.J., Thomson C.L., Jenkin M.E., Thetford R. and
764 Fitzgerald P., 2010. The ozone sourceereceptor model e A tool for UK ozone policy,
765 Atmospheric Environment , 44, 4283-4297.
766
767 Hough, A. M., 1988. The calculation of photolysis rates for use in global tropospheric
768 modelling studies, United Kingdom Atomic Energy Authority (UKAEA), Harwell Report
769 AERE H 13259.
770
771 Jenkin, M.E., Watson, L.A., Utembe, S.R. and Shallcross, D.E., 2008. A Common
772 Representative Intermediates (cri) mechanism for VOC degradation. Part 1: Gas phase
773 mechanism development, Atmospheric Environment , 42, 7185-7195.
774
775 Jones, A.M. and Harrison, R.M., 2011. Temporal trends in particulate sulphate
776 concentrations at European sites and relationships to sulphur dioxide, Atmospheric
777 Environment , 45, 873-882.
778
779 McMahon, T.A., 1979. Empirical Atmospheric deposition parameters – A survey,
780 Atmospheric Environment, 3, 571-585.
781
782 Metcalfe, S.E., Whyatt, J.D., Nicholson, J.P.G., Derwent, R.G. and Heywood, E., 2005.
783 Issues in model validation: assessing the performance of a regional-scale acid deposition
784 model using measured and modelled data, Atmospheric Environment , 39, 587-598.
785
786 Meij de, A., Thunis, P., Bessagnet, B. and Cuvelier, C., 2009. The sensitivity of the
787 CHIMERE model to emissions reduction scenarios on air quality in Northern Italy,
788 Atmospheric Environment, 43, 1897-1907.
789
790 Monteiro, A., Miranda, A.I., Borrego, C., Vautard, R., Ferreira, J. and Perez, A.T., 2007.
791 Long-term assessment of particulate matter using CHIMERE model, Atmospheric
792 Environment, 41, 7726-7738.
793
794 Nath, S. and Patil, R.S., 2006. Prediction of air pollution concentration using an in situ real
795 time mixing height model, Atmospheric Environment, 40, 3816–3822
796
797 Nenes, A., Pandis, S.N. and Pilinis, C., 1998a. ISORROPIA: A new thermodynamic
798 equilibrium model for multiphase multicomponent inorganic aerosols, Aquatic
799 Geochemistry, 4, 123-152.
800
801 Nenes, A., Pilinis, C., and Pandis, S.N., 1998b. Continued development and testing of a
802 new thermodynamic aerosol module for urban and regional air quality models,
803 Atmospheric Environment, 33, 1553-1560.
804
805 Passant, N.R. (2002) Speciation of UK Emissions of Non-Methane Volatile Organic
806 Compounds, AEA Technology, Report No. AEAT/ENV/R/0545 Issue 1
807
808 PELCOM (2000), Final Report on the Pan-European Land Cover Monitoring project
809 (PELCOM), funded by the European Commission DGXII (ENV4-CT96-0315).
810 Report edited by C.A. Mücher and available from
811 http://www.geoinformatie.nl/projects/pelcom/public/index.htm
812
813 Redington, A.L. and Derwent, R.G., 2002. Calculation of sulphate and nitrate aerosol
814 concentrations over Europe using a Lagrangian dispersion model, Atmospheric

Environment, 36, 4425-4439.

Schaap, M., van Loon, M., ten Brink, H., Dentener, F.J., and Builtjes, P.J.H., 2004. Secondary inorganic aerosol simulations for Europe with special attention to nitrate, Atmospheric Chemistry & Physics, 4,857-874

Schaap, M., Timmermans, R.M.A., Sauter, F.J., Roemer, M., Velders, G.J.M., C Boersen, G.A., Beck, J.P. and Builtjes, P.J.H., 2008. The LOTOS-EUROS model: description, validation and latest developments, International Journal of Environment and Pollution, 32, 270 290.

Simpson, D., Benedictow, A., Berge, H., Bergstrom, R. Fagerli, H., Gauss, M., Hayman, G.D., Jenkin, M.W., Jonson, J.E., Nyiri, A, Semeena, V.S, Tsyro, S., Tuovinen, J.P., Valdebenito, A., and Wind, P.. 2011. The EMEP MSC-W chemical transport model. https://wiki.met.no/_media/emep/page1/userguide_062011.pdf

Smith, M.H., Park, P.M., Consterdine, I.E., 1993. Marine aerosol concentrations and estimated fluxes over the sea. Q.J.R. Meteorol. Soc., 119, 809-824.

Stern, R., Builtjes, P., Schaap, M., Timmermans, R., Vautard, R., Hodzic, A., Memmesheimer, M., Feldmann, H., Renner, E., Wolke, R. and Kerschbaumer, A., 2008. A model inter-comparison study focussing on episodes with elevated PM10 concentrations, Atmospheric Environment, 42, 4567-4588.

Stohl, A., 1998. Computation, Accuracy and Applications of Trajectories – A Review and Bibliography, Atmospheric Environment, 32, 947–966.

Sutton, M.A., Tang, Y.S., Miners, B. and Fowler D., 2001. A new diffusion denuder system for long term, regional monitoring of 5atmospheric ammonia and ammonium, Water, Air and Soil Pollution Focus, 1, 145-156.

Tang, Y.S, van Dijk, N., Anderson, M., Simmons, I., Smith, R.I., Armas-Sanchez, E., Lawrence, H. and Sutton, M.A., 2008. Monitoring of nitric acid, particulate nitrate and other species in the UK – 2007, Interim report under the UK Acid Deposition Monitoring Network to NETCEN/DEFRA.

Thunis, P., Rouil, L., Cuvelier, C., Stern, R., Kerschbaumer, A., Bessagnet, B., Schaap, M., Builtjes, P., Tarrason, L. Douros, J., Moussiopoulos, N., Pirovano, G. and Bedogni, M., 2007. Analysis of model responses to emission-reduction scenarios within the City Delta project, Atmospheric Environment, 41, 208-220.

Walker, H.L., Derwent, R.G., Donovan, R., and Baker, J., 2009. Photochemical trajectory modelling of ozone during the summer PUMA campaign in the UK West Midlands, Science of the Total Environment, 407, 2012-2023.

Watson, L.A., Shallcross, D.E., Utembe, S.R. and Jenkin, M.E., 2008. A Common Representative Intermediates (cri) mechanism for VOC degradation. Part 2: Gas phase mechanism reduction, Atmospheric Environment, 42, 7196-7204.

Wesely, M.L. and Hicks, B.B., 2000. A review of the current status of knowledge on dry deposition, Atmospheric Environment, 34, 2261-2282.

867 Whyatt, J.D., Metcalfe, S.E., Nicholson, J., Derwent, R.G., Page, T. and Stedman, J.R.,
868 2007. Regional scale modelling of particulate matter in the UK, source attribution and an
869 assessment of uncertainties, Atmospheric Environment, 41, 3315-3327.
870
871 Yin, J. and Harrison, R.M., 2008. Pragmatic mass closure study for $PM_{1.0}$, $PM_{2.5}$ and PM_{10}
872 at roadside, urban background and rural sites, Atmospheric Environment, 42, 980-988.

TABLES LEGENDS

Table 1. Summary of changes made to the UK-Photochemical Trajectory Model.

Table 2. Simple statistics calculated using modeled and measured concentrations collected over the period from 02/04/2007 to 30/04/2007. Mean temperature 284.3 ± 2.3K and relative humidity of 71.8 ± 6.7 %. [* Values represent the measured monthly value only. ** The O_3 values represent the period when measured values were available, from 26/04/2007 to 19/05/2007.]

Table 3. Model performance metrics for the period from 19/03/2007 to 19/05/2007 using full days data. [N = number of complete pairs of measured and calculated values; MB = mean bias (μg/m3); NMB = Normalised mean bias; MGE = mean gross error; NMGE = normalised mean gross error; FAC2 = A count fraction of points within 0.5 and 2 times the observation; RMSE = root mean square error (μg/m3); r = Spearman's correlation; r2 = correlation coefficient; and IA = Index of Agreement.]

Table 4. Observed changes in values of the Performance Metrics when each enhancement in the model is restored to its original setting.

Table 5. Change of calculated species concentrations (%) resulting from precursor abatement (by 30%) on the calculated chloride, nitrate and sulphate concentrations. A comparison is made with the study of Derwent et al. (2009) – abatement figures shown in italics.

FIGURE LEGENDS

Figure 1. Boundaries separating the Northern, Eastern, Southern, Western and Central Regions of Europe. Initial concentrations are specified for each region and are used as initial conditions in each calculation depending on which region the trajectory starts.

Figure 2. Comparison between calculated and measured PM_{10} chloride, nitrate and sulphate. Measurements (black line) were made with a Rupprecht and Patashnick Partisol 2025 sampler with PM_{10} sampling inlet. The calculated data is depicted by the blue whisker plots derived from the statistics of each group of 24 hourly calculated values. The middle horizontal line represents the median; the two hinges represent the first and third quartile; and the two whiskers represent the maximum and minimum values. Also included are the results shown by the brown line from the initial PTM model. (Referring to Figure 1, the coloured ribbon at the bottom of each plot shows the zone from which the trajectory used in the calculation started.)

Figure 3. Comparison between calculated and measured PM10 chloride, nitrate and sulphate. Measurements made with a Rupprecht and Patashnick Partisol 2025 sampler with PM_{10} sampling inlet. The data is fitted using the Reduced Major Axis method (Ayers, 2001), indicated by the solid black line and equation. Also included on these correlation plots is the ideal case of a 1:1 correlation marked out by the blue line and the boundaries where the calculated values are twice or half the value of the measured values (dashed lines).

Table 1. Summary of changes made to the UK-Photochemical Trajectory Model.

	Enhancement of	TO	FROM
Emissions	Continental VOC/NOx/CO/SO2/ Biogenics/NH3	EMEP, base year 2005 (50×50 km)	CORINAIR, base year 1985 (150×150 km)
	United Kingdom VOC/NOx/CO/SO2/ Biogenics/NH3	NAEI, base year 2005, (10×10 km)	CORINAIR, base year 1985 (10×10 km)
	Sea Salt flux	Gong (2003) parameterisation	None present
	Boundary layer / free troposphere injection	B.L. height determines input of SO_2 and NO_X.	None present
	Initial Conditions	Dependent on initial lat/long position being in either a N/E/S/W or Central Region.	Westerly Clean conditions for all trajectories
Chemical Mechanism	Gas phase	cri-v02	MCM
	Aqueous phase	ISORROPIA II	None present
	Aqueous oxidation of SO_2,	Schaap et al. (2004)	None present
	Photolysis Rates	Dependent of lat/long, cloud cover and surface.	Based on a parameterisation.
	Gaseous dry deposition Rates	Dependent on surface (land/sea)	Fixed values
	NO_2 & SO_2 wet deposition Rates	McMahon et al. (1979) parameterisation	None Present
	PM deposition rates	Smith et al. (1993) parameterisation	None present
Back Trajectory Calculation	Lat/Long	Calculated using HYSPLIT	Calculated using BADC
	Mixing Depth	Calculated using HYSPLIT	Saw tooth fn
	Temperature	Calculated using HYSPLIT	Sinusoidal fn
	RH	Calculated using HYSPLIT	Sinusoidal fn
	Cloud Cover	Calculated using HYSPLIT	None present
	U10	Calculated using HYSPLIT	None present
	Rain	Calculated using HYSPLIT	None present
	(YY/MM/DD/HH/MM)	Calculated using HYSPLIT	None present

Table 2. Simple statistics calculated using modeled and measured concentrations collected over the period from 02/04/2007 to 30/04/2007. Mean temperature 284.3 ± 2.3K and relative humidity of 71.8 ± 6.7 %. [* Values represent the measured monthly value only. ** The O_3 values represent the period when measured values were available, from 26/04/2007 to 19/05/2007].

Const-ituent	Unit	Field Values					PTM Values				
		Min.	*Lower quartile*	**Geo. Mean**	*Upper quartile*	*Max.*	*Min.*	*Lower quartile*	**Geo. Mean**	*Upper quartile*	*Max.*
$NH_{3(g)}$	ppb	-	-	6.95	-	-	*0.14*	*3.95*	**6.11**	*9.8*	*22.1*
NH_4^+	$\mu g/m^3$	-	-	2.80	-	-	*0*	*0*	**2.80**	*5.05*	*16.9*
HNO_3	ppb	-	-	0.59	-	-	*0*	*0.02*	**0.07**	*0.28*	*2.3*
SO_2	ppb	-	-	0.99	-	-	*0.02*	*0.12*	**0.27**	*0.63*	*15.9*
HCl	ppb	-	-	0.26	-	-	*0*	*0*	**0.01**	*0.04*	*0.99*
Cl^-	$\mu g/m^3$	*0.13*	*0.26*	**0.56**	*1.10*	*3.40*	*0*	*0.43*	**0.67**	*1.42*	*4.16*
NO_3^-	$\mu g/m^3$	*2.17*	*4.56*	**6.89**	*10.7*	*16.4*	*0.05*	*4.62*	**7.45**	*13.9*	*35.7*
SO_4^{2-}	$\mu g/m^3$	*1.21*	*2.42*	**3.62**	*5.33*	*9.92*	*0.48*	*1.59*	**4.27**	*9.39*	*67.8*
CO	ppb	-	-	-	-	-	*123.6*	*150*	**177.1**	*200.8*	*528.5*
NO	ppb	*0.00*	*0.00*	**1.20**	*2.20*	*18.8*	*0.0*	*0.03*	**0.43**	*2.64*	*115.0*
NO_2	ppb	*0.00*	*3.67*	**7.03**	*9.98*	*37.1*	*0.47*	*2.46*	**3.78**	*5.93*	*20.2*
O_3^{**}	ppb	*7.6*	*24.4*	**28.7**	*36.7*	*62.1*	*0*	*15.8*	**23.0**	*28.4*	*46.3*

Table 3. Model performance metrics for the period from 19/03/2007 to 19/05/2007 using full days data. [N = number of complete pairs of measured and calculated values; MB = mean bias (μg/m^3); NMB = Normalised mean bias; MGE = mean gross error; NMGE = normalised mean gross error; FAC2 = A count fraction of points within 0.5 and 2 times the observation; RMSE = root mean square error (μg/m^3); r = Spearman's correlation coefficient; and IA = Index of Agreement.]

	Chloride	*Nitrate*	*Sulphate*
Observed Values			
Arithmetic Mean	1.10	6.75	3.90
St dev	1.02	6.23	2.60
Original Model Values			
Arithmetic Mean	-	2.96	1.73
St dev	-	4.99	4.11
N		58	58
MB	-	-3.93	-2.24
MGE	-	5.10	3.33
NMB	**-**	**-0.59**	**-0.58**
NMGE	-	0.76	0.86
RMSE	-	6.80	4.43
FAC2		**0.18**	**0.11**
r (Spearman)	-	0.57	0.55
IoA	-	0.88	0.86
Enhanced Model Values			
Arithmetic Mean	0.96	6.85	4.03
St dev	0.52	5.10	3.33
N	57	57	57
MB	-0.11	0.32	0.28
MGE	0.78	2.47	1.82
NMB	**-0.10**	**0.05**	**0.07**
NMGE	0.71	0.36	0.47
RMSE	1.06	3.94	2.51
FAC2	**0.42**	**0.77**	**0.81**
r (Spearman)	0.27	0.83	0.65
IA	0.9	0.96	0.95

Table 4. Observed changes in values of the Performance Metrics when each enhancement in the model is restored to its original setting.

	Δ (Arithmetic Mean)			*Δ NMB*		
Enhanced Model Values minus...	*Cl^-*	*NO_3^-*	*SO_4^{2-}*	*Cl^-*	*NO_3^-*	*SO_4^{2-}*
HYSPLIT temp, RH, BLH values	14%	10.0%	-8.2%	-0.08	-0.18	0.00
Enhanced photolysis rates	-7.4%	-17%	-0.5%	0.15	0.12	-0.09
ISORROPIA II	-	8.0%	0.9%	0.11	0.09	0.01
Aqueous oxidation of SO_2,	2.1%	2.7%	-30%	0.01	0.03	-0.33
Trajectory dependent initial conditions	4.3%	-0.3%	-26%	-0.02	-0.01	0.22
NO_2 and SO_2 Stack height dependent emissions	-2.1%	-1.9%	14%	0.03	0.00	-0.29
Cloud cover dependent photolysis rates (sunny day scenario)	-1.1%	6.4%	0.9%	-0.01	0.07	0.01

Table 5. Change of calculated species concentrations (%) resulting from precursor abatement (by 30%) on the calculated chloride, nitrate and sulphate concentrations. A comparison is made with the study of abatement figures shown in italics.

Precursor Abated	*Chloride*	*Nitrate*	*Sulphate*	Σ (chloride + nitrate + sulphate)	*PM_{10}*
NH3	-2.2	-5.1 *(-12.2)*	0.1 *(0)*	-3.1	-1.6
NOx	-0.6	-17.7 *(-14.8)*	1.9 *(2.3)*	-8.5	-3.7
SO2	0.8	2.5 *(3.5)*	-20.8 *(-14.8)*	-6.1	-2.3

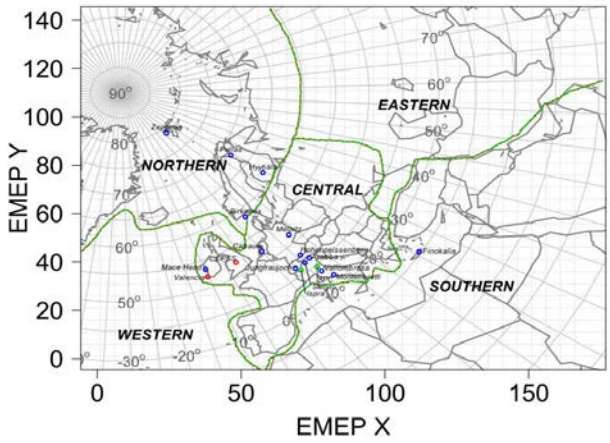

Figure 1. Boundaries separating the Northern, Eastern, Southern, Western and Central Regions of Europe. Initial concentrations are specified for each region and are used as initial conditions in each calculation depending on which region the trajectory starts.

960
961

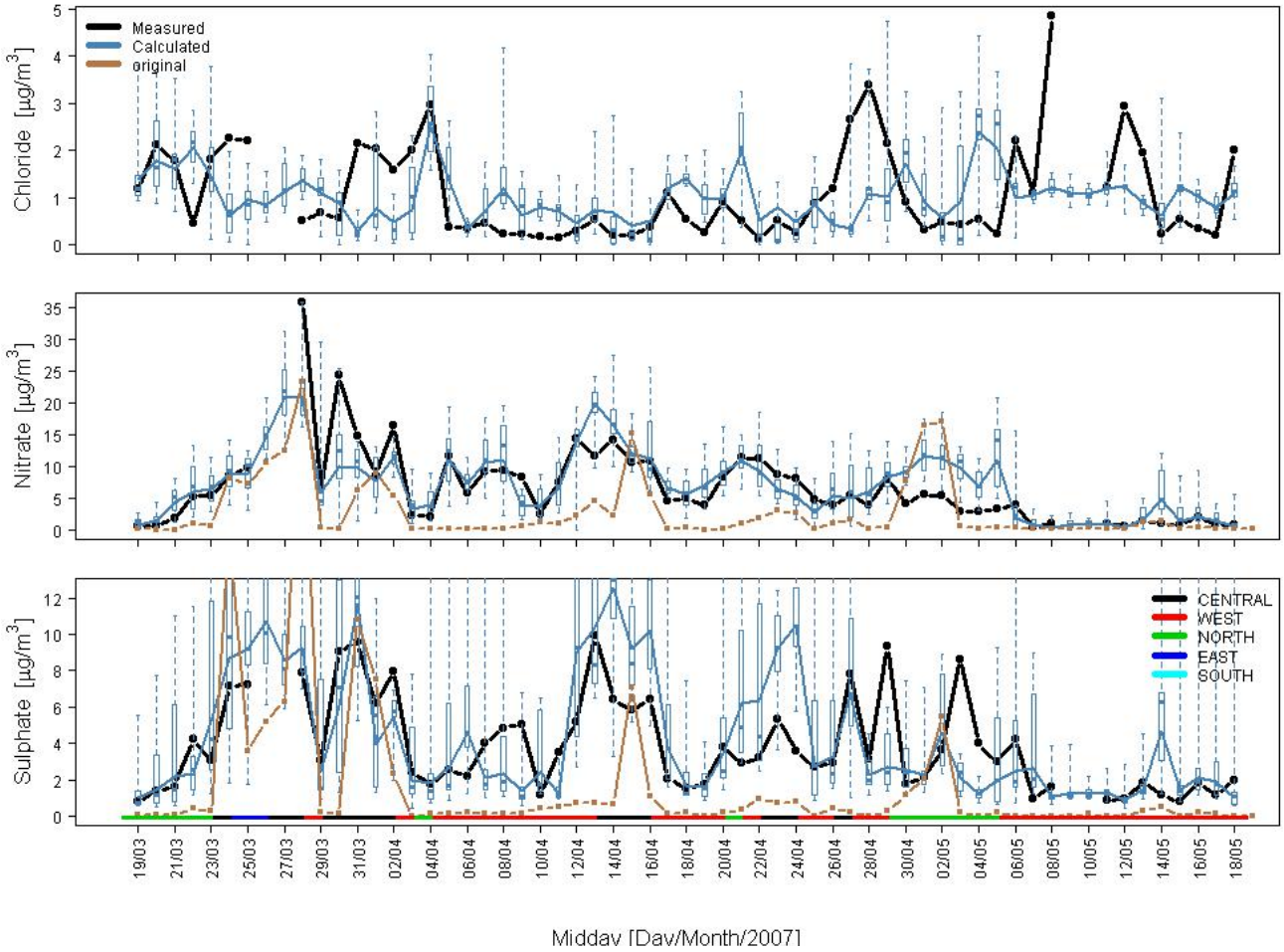

Figure 2. Comparison between calculated and measured PM_{10} chloride, nitrate and sulphate. Measurements (black line) were made with a Rupprecht and Patashnick Partisol 2025 sampler with PM_{10} sampling inlet. The calculated data is depicted by the blue whisker plots derived from the statistics of each group of 24 hourly calculated values. The middle horizontal line represents the median; the two hinges represent the first and third quartile; and the two whiskers represent the maximum and minimum values. Also included are the results shown by the brown line from the initial PTM model. (Referring to Figure 1, the coloured ribbon at the bottom of each plot shows the zone from which the trajectory used in the calculation started.)

962

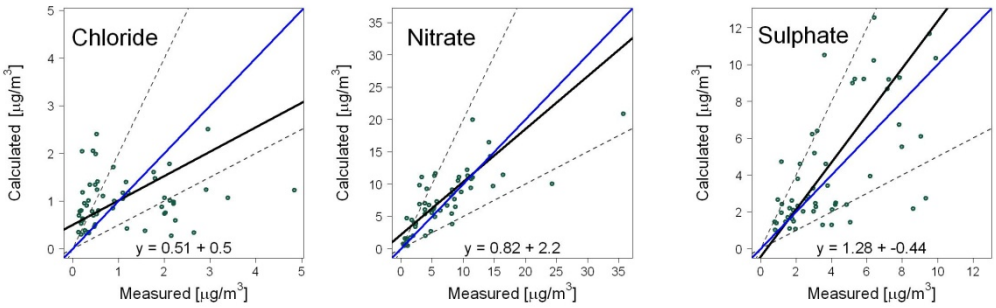

Figure 3. Comparison between calculated and measured PM_{10} chloride, nitrate and sulphate. Measurements made with a Rupprecht and Patashnick Partisol 2025 sampler with PM_{10} sampling inlet. The data is fitted using the Reduced Major Axis method (Ayers, 2001), indicated by the solid black line and equation. Also included on these correlation plots is the ideal case of a 1:1 correlation marked out by the blue line and the boundaries where the calculated values are twice or half the value of the measured values (dashed lines).

963
964